

The use of hyperspectral remote sensing for mineral exploration: a review

Enton Bedini*

*Geological Survey of Denmark and Greenland (GEUS), Øster Voldgade 10, 1350 Copenhagen K, Denmark.
Email: enton_bedini@hotmail.com (Corresponding author)

Received 14 October 2017; accepted 15 November 2017

Abstract

The hyperspectral remote sensing technology has been available to the research community for more than three decades. Since in its first steps the hyperspectral technology was also promoted as a tool for mineral exploration. Numerous mineral exploration applications of hyperspectral remote sensing have been reported. This paper provides an up-to-date and focused review of the applications of the hyperspectral remote sensing to mineral exploration. The ore deposits are grouped based on major processes of formation (magmatic, hydrothermal, sedimentary, supergene). The review shows that the hyperspectral remote sensing technology has found application to the study and exploration of a number of ore deposits including kimberlites (host-rocks of diamonds), carbonatites (host-rock of rare earth elements deposits), porphyry deposits, epithermal gold and silver deposits, skarn deposits, volcanic-hosted massive sulfide (VHMS) deposits, orogenic gold deposits, Carlin-type gold deposits, SEDEX Pb-Zn-Ag deposits. On the other hand, the possibilities of the hyperspectral technology remain still underexplored for the study and exploration of chromite deposits, Ni-sulfide deposits in mafic and ultramafic rocks, rare-metal pegmatites, greisen and related deposits, Mississippi Valley-type (MVT) Pb-Zn deposits, Kupferschiefer deposits and uranium deposits in sedimentary basins, iron ores in banded-iron formations, laterites and bauxites. A special attention has been paid in this review to the applications in mineral exploration of the emerging airborne hyperspectral thermal infrared technology. In addition, the possibilities and limitations of spaceborne hyperspectral imagery of moderate spatial resolution for detailed characterization and detection of mineralized systems are discussed for each major deposit type. The spatial resolution of the hyperspectral data is noted to be a key factor on the success of a hyperspectral exploration project. By providing a full up-to-date picture of the applications and contribution of the hyperspectral imagery to the exploration and characterization of ore deposits this review paper should be useful to the interested geological remote sensing researcher and practitioner, and to the mineral exploration manager as well.

Keywords: hyperspectral remote sensing, airborne imagery, spaceborne imagery, mineral exploration, ore deposits

Resumo

1. Introduction

Remote sensing is the science of acquiring, processing, and interpreting images and related data, acquired from aircraft and satellites, that record the interaction between matter and electromagnetic energy (Sabins, 1997). The visible to short wave infrared (0.4-2.5 μm), and the thermal infrared (8-12 μm) regions of the electromagnetic spectrum provide mineralogic information due to electronic transitions and vibrational processes in minerals (e.g. Hunt, 1982; Clark, 1999; Christensen et al., 2000). These wavelength regions of the electromagnetic spectrum are invaluable to the geological remote sensing, as the atmosphere allows in these wavelength regions also the acquisition of

spectral information from a distance of several km-s (airborne platforms) to a distance of hundreds of km-s (satellite platforms) (e.g. Vincent, 1997; Sabins, 1999; van der Meer et al., 2012; Kruse, 2015).

Hyperspectral remote sensing is concerned with the acquisition of contiguous reflectance and emittance spectra from sensors mounted on airborne and spaceborne platforms. The emergence of hyperspectral image data to remotely map minerals on the surface of the Earth is the result of decades of laboratory, engineering and physics research conducted by both commercial and government sectors (Taranik and Aslett, 2009). A synopsis of major events which culminated in the development of mature hyperspectral

reflectance and thermal emissivity data collection capabilities that are currently available in worldwide capacity is provided by Taranik and Aslett (2009).

The hyperspectral sensors, measuring hundreds of spectral bands from aircraft and satellite platforms, provide unique spatial/spectral datasets for analysis of surface mineralogy (e.g. Goetz et al., 1985; Kruse et al., 2003). The hyperspectral technology since in its first steps was applied to mineral exploration (e.g. Goetz and Srivastava, 1985; Kruse, 1988). In more than three decades of applied hyperspectral remote sensing (Goetz, 2009), numerous mineral exploration studies have been reported. Although sometimes reluctant, the mineral exploration industry is increasingly incorporating hyperspectral imagery in exploration projects.

While the hyperspectral imaging is still overwhelmingly based on the airborne platforms, the use of space for the acquisition of hyperspectral imagery will make this technology more available to the interested researchers and users. This will increase the use of hyperspectral imagery in geology and also bring new insights to mineral exploration studies. Especially, the planned NASA's HySpiri spaceborne hyperspectral imagery with a swath of 500 km has the potential to be a breakthrough for the hyperspectral remote sensing of the Earth's surface (e.g. Kruse et al., 2011; Lee et al., 2015). Currently, the only freely available hyperspectral data from spaceborne sensors are provided from the NASA's Hyperion EO-1 (Ungar et al., 2003).

There are several review papers on the topic of geological remote sensing (e.g. Sabins, 1999; van der Meer et al., 2014), mineral mapping using hyperspectral data (e.g. Kruse, 2012), and hyperspectral data processing in geological and mineral exploration studies (e.g. Cloutis, 1996; Asadzadeh and de Souza, 2016). However, a focused and up-to-date review paper on the applications of hyperspectral

remote sensing in mineral exploration and ore deposit characterization is needed to better orient future research and applications.

This paper reviews the applications of hyperspectral remote sensing imagery acquired from airborne and spaceborne platforms to the exploration and characterization of major mineral deposit types. The ore deposits are grouped following a schema generally based on major processes of formation (magmatic, hydrothermal, sedimentary, supergene) (e.g. Ridley, 2013). In addition to studies published in peer reviewed journals are also cited conference papers or institutional reports when these are important to elucidate key aspects of the hyperspectral analysis of a certain type of mineralization. The paper also discusses the role that could play planned spaceborne hyperspectral sensors in the field of mineral exploration. This paper aims to provide an up-to-date reference for the use of hyperspectral remote sensing for mineral exploration and ore deposit characterization.

2. Infrared spectroscopy

The reflectance and emittance infrared spectra of minerals are well studied. An overview of the spectral reflectance characteristics of minerals is provided by Clark (1999). Examples of the reflectance spectra of several minerals are shown in Figure 1. The spectral emittance of minerals is presented in detail by Salisbury (1991) and Christensen et al. (2000). Examples of the emission spectra of several minerals in the 8-12 μm spectral region are shown in Figure 2.

The spectral libraries (e.g. Christensen et al., 2000; Clark et al., 2007; Baldrige et al., 2009; among others) contain reflectance and emittance infrared spectra for a large number of minerals and constitute an important reference source for the geological remote sensing analyst.

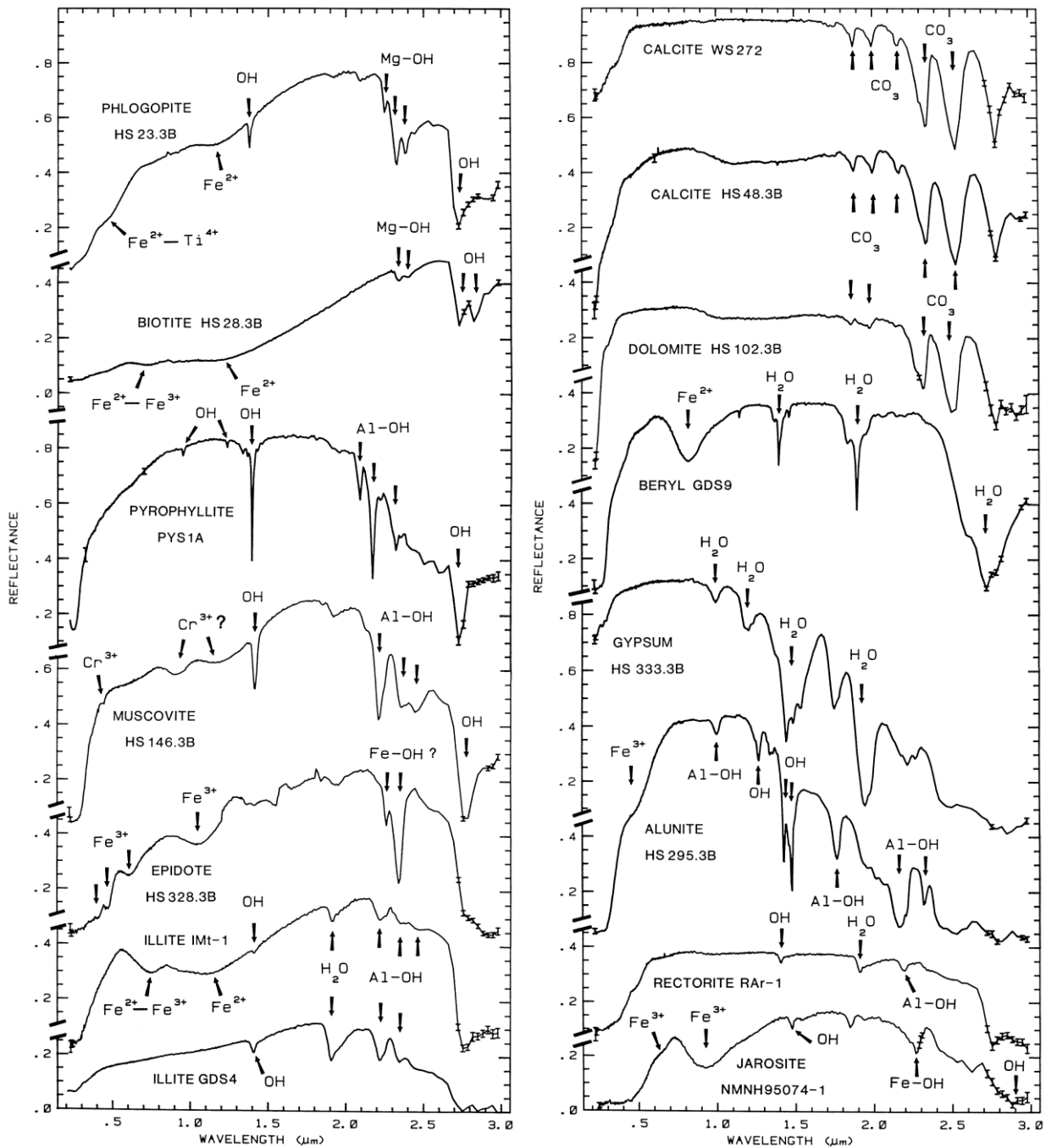


Figure 1 - Examples of reflectance spectra of minerals in the 0.4-3 μm wavelength region (from Clark 1999).

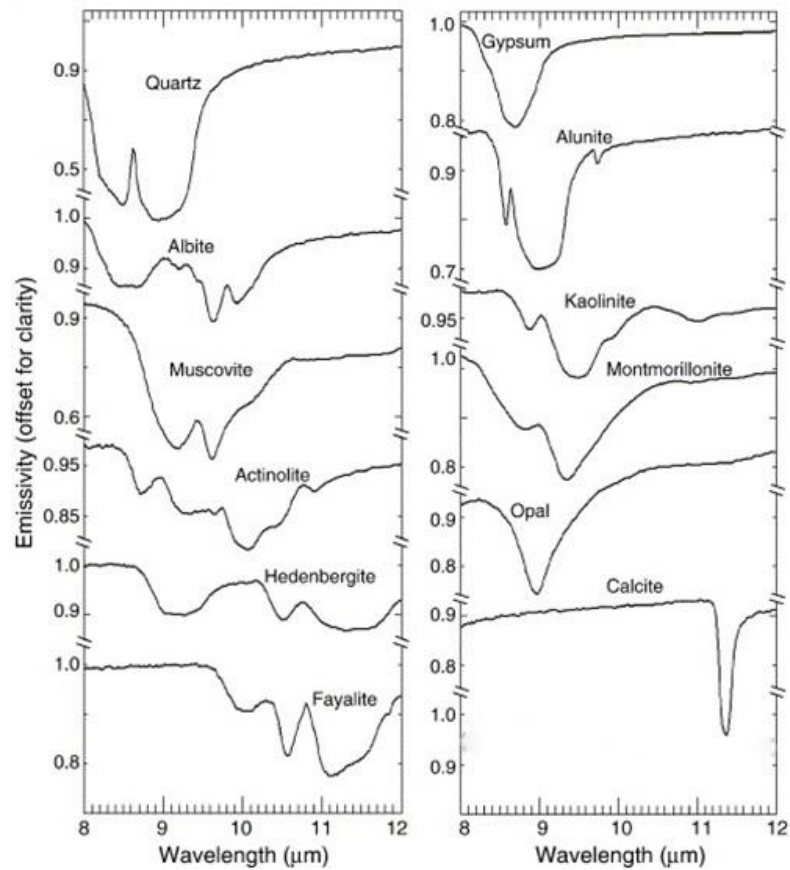


Figure 2 - Examples of emissivity spectra of minerals in the 8-12 μm wavelength region (from Vaughan et al. 2005).

3. Hyperspectral remote sensing of minerals

Hyperspectral remote sensing combines two sensing modalities: imaging and spectroscopy. An imaging system captures a picture of a remote scene related to the spatial distribution of the power of reflected and/or emitted electromagnetic radiation integrated over some spectral band (Eisman, 2012). On the other hand, spectroscopy measures the variation in power with the wavelength or frequency of light, capturing information related to the chemical composition of the materials measured. The instrumentation used to capture such spectral information is called an imaging spectrometer or a hyperspectral sensor (Figure 3).

The minerals that have diagnostic spectral reflectance or emission features, and that crop out on the surface can be detected, and their spatial

distribution can be mapped by the analysis of the data acquired by the hyperspectral sensors (e.g. Figures 4, 5).

The hyperspectral sensors can be mounted on airborne platforms (airborne hyperspectral remote sensing) or on spaceborne platforms (satellite hyperspectral remote sensing). The era of hyperspectral remote sensing began with the development at the Jet Propulsion Laboratory of the Airborne Imaging Spectrometer (AIS) (Vane et al. 1984). The widely used Airborne Visible/Infrared Imaging Spectrometer (AVIRIS) represents the second generation of NASA hyperspectral sensors (Vane et al., 1993; Green et al., 1998; Goetz, 2009). AVIRIS records spectral reflectance in 224 narrow bands covering the 0.4-2.5 μm spectral range. The AVIRIS has usually recorded data with a spatial resolution of 4 m up to 20 m.

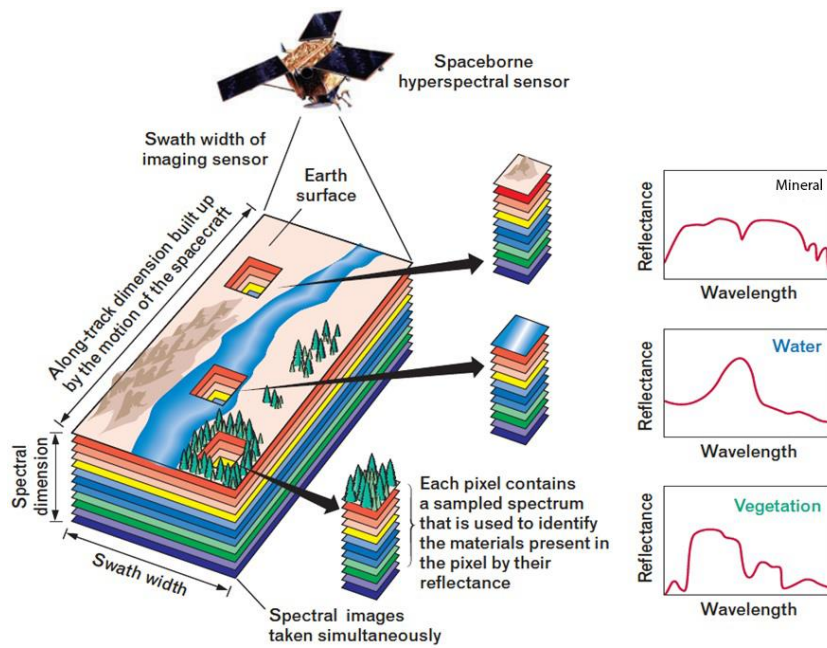


Figure 3 - The concept of hyperspectral imaging. At each pixel is recorded a spectral measurement of the reflectance, which can be interpreted to identify the materials present in it. The imaging spectrometer (or the “hyperspectral sensor”) can be mounted on airborne or spaceborne platforms. Modified from Shaw and Burke (2003).

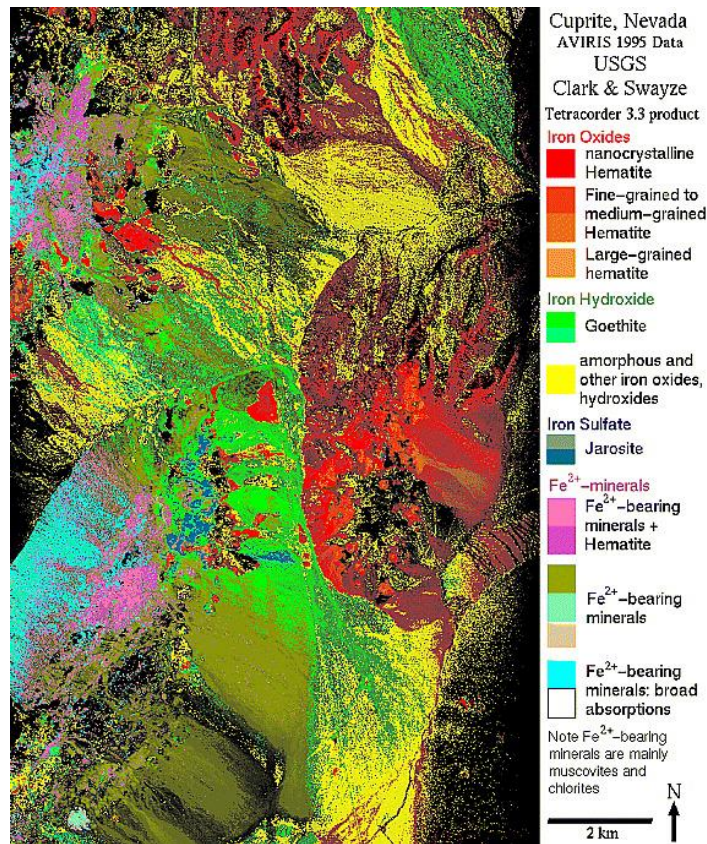


Figure 4 - Mapping results from the analysis of visible to near infrared (VNIR) AVIRIS airborne hyperspectral imagery over Cuprite, Nevada (from Clark et al., 2003).

A breakthrough in making airborne hyperspectral data available to exploration companies and to a larger number of researchers was the development by Integrated Spectronics in Australia of the Hyperspectral Mapper (HyMap™) imaging system. The HyMap records spectral reflectance in 126 narrow spectral bands covering the 0.4-2.5 μm spectral range (Cocks et al., 1998). The HyMap in general has recorded hyperspectral data with a spatial resolution of

about 4 m.

On the other hand, the emerging technology of airborne hyperspectral thermal infrared imaging is bringing new insights to geological and mineral exploration studies (e.g. Cudahy, 2016; Vaughan et al., 2003). The reason for this is that several important minerals including quartz and feldspars display diagnostic spectral features only in the thermal infrared wavelength region.

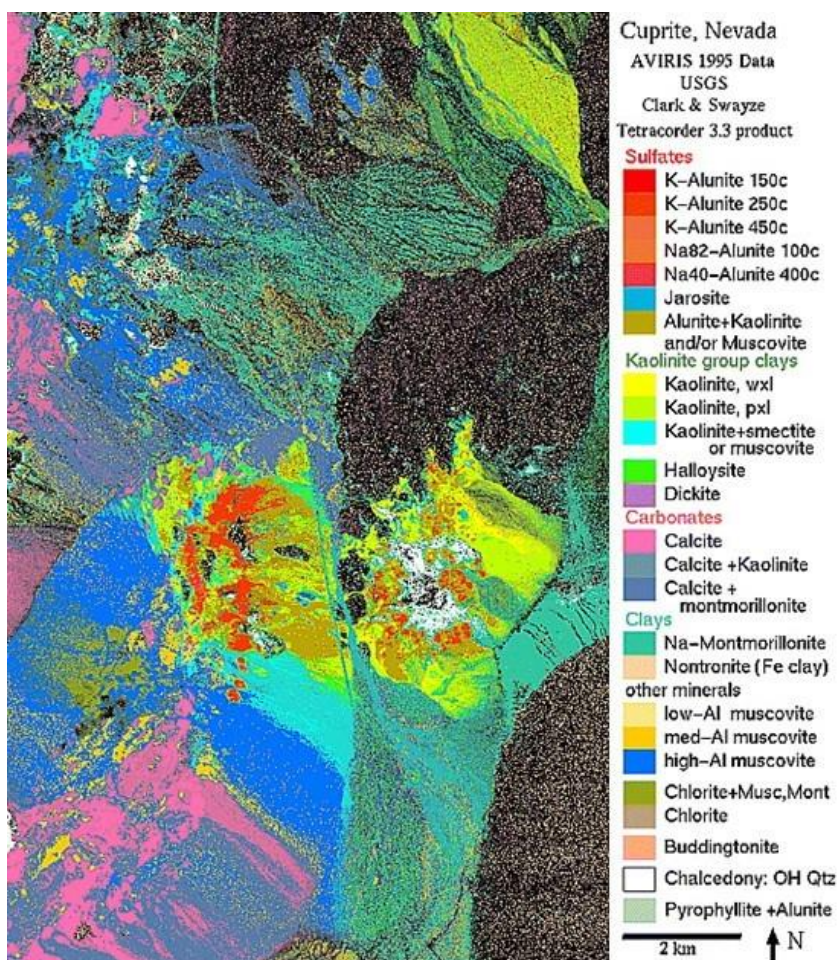


Figure 5. Mapping results from the analysis of short-wave infrared (SWIR) AVIRIS airborne hyperspectral imagery over Cuprite, Nevada (from Clark et al. 2003).

An airborne hyperspectral survey can reveal zoning patterns and distinct mineral assemblages that may take years to find (or may never be found) with other methods (Bedell, 2004). However, given the time and cost of airborne hyperspectral surveys, these are best applied where commitments to the property and district are strong (Bedell, 2004).

Currently, there have been developed a large number of airborne and spaceborne hyperspectral

sensors and others are being planned (Eisman, 2012). The acquisition of high-quality hyperspectral data from satellites will open new frontiers to the application of hyperspectral remote sensing to mineral exploration (e.g. Kruse et al., 2011). However, the spatial resolution of the planned spaceborne hyperspectral reflectance data will be moderate (30 m), a factor that may diminish the application of such data to detailed mineral detection and mapping.

4. Hyperspectral remote sensing for mineral exploration

This section reviews the literature related with the application of hyperspectral remote sensing to mineral exploration. The ore deposits are grouped based on the major genetic process of enrichment as follows: magmatic – concentration as a result of chemical and mineralogical processes in magmas; hydrothermal – concentration as a result of precipitation from heated aqueous fluids migrating through crustal rocks; sedimentary – concentration by mechanical or chemical processes at the time of sedimentation; supergene – enrichment as a result of weathering processes (Ridley, 2013).

4.1 Magmatic ore deposits

Diamonds in kimberlites

Primary diamond ores occur in unique, rare and small-volume potassic ultrabasic rocks, which as a class are known as kimberlitic rocks. They occur as diatremes, dykes and small pipe-shaped intrusive bodies. Commonly they contain macrocrysts set in a fine-grained matrix. Olivine is the dominant member of the macrocryst assemblage. The matrix minerals include olivine, phlogopite, perovskite, spinel, chromite, diopside, apatite, calcite, and serpentine. The replacement of early-formed olivine, phlogopite and apatite by serpentine and calcite is common (e.g. Mitchell, 1986).

Studies on the spectral reflectance characteristics of kimberlites indicate that serpentine, calcite, phlogopite, chlorite, talc, smectite and saponite are the main minerals to be targeted from the hyperspectral data for the detection of the surface outcrop of kimberlites (e.g. Tukiainen et al., 2003; Hauff, 2009). The use of hyperspectral remote sensing for the detection of kimberlites has been reported in several publications (Kruse and Boardman, 2000; Keeling et al., 2004; Tukianien and Thorning, 2005; Suryanarayana Rao et al., 2013).

Kruse and Boardman (2000) used airborne AVIRIS and HyMap hyperspectral data to map Devonian-age diamondiferous kimberlitic diatremes in a district between Colorado and Wyoming. Tukianien and Thorning (2005) used HyMap data to prospect for kimberlite dykes in the area of Søndre Strømfjord in central West Greenland. A number of previously unknown kimberlite dykes were detected. Keeling et al. (2004) report that in their target area in Terowie district in southern Australia, the rate of kimberlite finding using coincident hyperspectral and magnetic data was

considerably improved. This indicates the benefits of geophysical and hyperspectral remote sensing data integration in the exploration for kimberlites.

Research and case studies using airborne hyperspectral thermal infrared data will give new insights to the remote sensing of such a particular rock type, as also indicated by thermal infrared spectral imaging of kimberlite drill cores (e.g. Tappert et al., 2015). The moderate spatial resolution (30 m) of spaceborne hyperspectral data is an important limitation for the detection of kimberlites (e.g. Guha et al., 2013).

Economic mineralization related with carbonatites and alkaline intrusions: rare earth elements, niobium, etc.

The carbonatites are defined in the IUGS system of classification as igneous rocks composed of more than 50 modal per cent primary (i.e., magmatic) carbonate and containing less than 20 wt % SiO₂ (Le Maitre, 2002). Carbonatites are an important source of rare earth elements, niobium and also thorium and uranium could occur in economic concentrations (e.g. Verplanck et al., 2014).

Rowan et al. (1986) analyzed samples from four carbonatite complexes in the U.S.A using infrared spectroscopy techniques. The study showed that the carbonatite rocks and related alkaline lithologies contain a series of minerals with well-defined spectral absorption features. In addition, the study gave examples of the absorption features in the visible and near-infrared (VNIR) wavelength region of rare earth elements (REE). It was observed that a content of more than 300 ppm Nd produces absorption features in the reflectance spectra (Rowan et al., 1986). A detailed reflectance spectroscopy study for the detection of rare earth elements in samples of carbonatites from different parts of the world is carried out by Neave et al. (2016). Boesche et al. (2015) have shown that close-range hyperspectral imaging is useful to detect absorption features caused by the rare earth elements.

Rowan et al. (1995) analyzed airborne hyperspectral data recorded by the AVIRIS imaging system at the Iron Hill carbonatite complex in Colorado. They report the detection of carbonatite and alkaline lithologies, and the detection of carbonatite dykes in an area prospective for REE. This area has also anomalous thorium contents. Bedini (2009) analyzed airborne HyMap data of the Sarfartoq carbonatite complex in southern West Greenland. The hyperspectral data mapped several lithologies, among others calcite carbonatite occurrences (enriched in rare earth elements) within a predominantly dolomite carbonatite outcrop of the core zone. Bedini and

Rasmussen (2017) also used HyMap data to map carbonatite dykes in the margin of the Sarfartoq carbonatite complex in a zone that has anomalous thorium contents. The area is prospective for REE mineralization and a number of drillings have been carried out. In the same study, Bedini and Rasmussen (2017) noted that a niobium deposit (pyrochlore mineralization) does not show absorption features that could unequivocally be assigned to the mineralization. Zimmermann et al. (2016) used hyperspectral data to characterize the Epembe carbonatite-hosted Nb-Ta-LREE deposit in Namibia. They report the detection from the hyperspectral data of potential enrichment zones. Rowan et al. (1996) analyzed AVIRIS data of an area which encompasses the Mountain Pass Carbonatite complex in California. The same area was mapped in another study with AVIRIS and spaceborne multispectral ASTER data indicating the role of spaceborne remote sensing for lithologic mapping of carbonatite complexes (Rowan and Mars, 2003). The Khanneshin carbonatite, in Afghanistan has also been investigated using airborne HyMap hyperspectral data (Kokaly and Johnson, 2011) and spaceborne multispectral ASTER data (Mars and Rowan, 2011).

Studies for the localization of carbonatite occurrences should in general be carried out by analysis of spaceborne imagery. However, airborne hyperspectral data are needed for detailed district level mineral exploration of known carbonatite complexes. Research on the benefits of the airborne hyperspectral thermal infrared imagery for the exploration of carbonatites would be a contribution to the geological remote sensing literature.

Chromite deposits and Ni-sulfide deposits in mafic and ultramafic rocks

Two common types of chromite deposits are recognised on the basis of ore-body form and their geological environment: stratiform chromite deposits in large, layered ultramafic–mafic intrusions; and podiform chromite ores in ophiolites or ‘Alpine peridotites’ (e.g. Ridley, 2013). Chromites and spinels display characteristic infrared reflectance spectra (Cloutis et al., 2004). However, on terrestrial remote sensing the prospection for chromitites is mainly based on the detection of the rock units where they occur (e.g. Pour et al., 2015).

Hyperspectral remote sensing investigations of the stratiform chromite deposits in large layered ultramafic-mafic intrusions have not been reported. A laboratory spectral thermal infrared imaging example of the chromite mineralization at Kemi, Finland is carried out by Kuosmanen et al. (2015). Livo and

Johnson (2011) report the results of HyMap hyperspectral data analysis for podiform chromite detection in the Aynak-Logar Valley, Afghanistan. The area containing the podiform chromite mineralization hosted within pre-Eocene ultramafic rocks was mapped in the HyMap data as ferrous and ferric iron-rich serpentine-bearing rocks. The mapping of ophiolite lithologies in Oman using hyperspectral data has shown interesting results that could also be useful to the exploration activities (Clenet et al., 2010).

The nickel sulphide deposits are associated with mafic and ultramafic rocks. The mineralogy of these deposits is usually simple, consisting of pyrrhotite, pentlandite, chalcopyrite and magnetite (Evans, 2013). Hyperspectral remote sensing prospection for Ni-Cu-PGE mineralization have focused on the mapping of mafic-ultramafic lithologies (e.g. Rogge et al., 2014).

The exploration for magmatic deposits (e.g. chromite deposits, nickel sulfide deposits) in mafic and ultramafic rocks, using hyperspectral imagery is a challenging field of research and more studies will be carried out as the availability of airborne and spaceborne hyperspectral data to interested researchers increases.

Rare-metal pegmatites

The term pegmatite is normally used to describe a coarse-grained granitic rock. In ore deposit geology, the interest in pegmatites is in the rare-metal pegmatites. Rare-metal pegmatites are of economic interest as ores of Ta, Sn, Cs, U, Rb, Li and Be. Pegmatite bodies vary greatly in size and shape. They range from pegmatitic schlieren and patches in parent granites, through thick dykes many kilometres long and wholly divorced in space from any possible parent intrusion, to pegmatitic granite plutons many kilometres squared in area (Evans, 1993).

There are few hyperspectral remote sensing studies of pegmatite rocks. Oshigami et al. (2013) analyzed HyMap data from southern Namibia. Among others they mapped high aluminum muscovite and lepidolite (lithium-bearing mica) from the airborne hyperspectral data. In an another study, analyzing the same HyMap data, Momose et al. (2011) conclude that in an arid environment the detection and mapping of the spatial distribution of pegmatites was possible using airborne hyperspectral data.

4.2 Hydrothermal ore deposits (magmatic environments)

Porphyry copper and molybdenum deposits

The porphyry deposits are extensively studied (e.g. Pirajno, 2009; and references therein). The three most important commodities by value worldwide in these deposits are Cu, Mo and Au. In the porphyry copper deposits the most important copper minerals are chalcopyrite and bornite, and more rarely chalcocite. Molybdenite is the only primary molybdenum ore mineral of porphyry molybdenum deposits. Hydrothermal wall-rock alteration is a characteristic component of porphyry deposits. Porphyry copper deposits are typically associated with very large hydrothermal alteration zones such as potassic, phyllic, argillic, and propylitic (Lowell and Guilbert, 1970).

The potassic, phyllic, argillic, and propylitic alteration zones of porphyry copper deposits contain alteration minerals with distinct spectral absorption features (Thompson et al., 1999) that provided they crop out on the surface, can be detected and mapped using multispectral and hyperspectral remote sensing imagery (e.g. Spatz, 1996; Tangestani and Moore, 2002; Berger et al., 2003; Mars and Rowan, 2006; Riley et al., 2009; Pour and Hashim, 2012; among others).

Berger et al. (2003) used AVIRIS hyperspectral data to map mineral alteration associated with two concealed porphyry copper deposits (Red Mountain and Sunnyside deposits) in the northern Patagonia Mountains of Arizona. The AVIRIS data analysis mapped alteration minerals related with three alteration zones: phyllic, argillic and propylitic. The AVIRIS mapping results provided new information for the alteration zones compared to what was previously mapped in the field (Berger et al., 2003). The mineralogy of a leach cap zone over a sub-economic Mo-Cu porphyry deposit in the Grizzly Peak caldera in the central Colorado Rocky Mountains was investigated by hyperspectral data by Coulter et al. (2009). The hyperspectral data mapped mixtures of jarosite, goethite and hematite and clay minerals that characterize the alteration (sericite, kaolinite, dickite and pyrophyllite).

The porphyry molybdenum deposits have many features in common with porphyry copper deposits. The alteration patterns are very similar to those found in porphyry copper deposits, with potassic alteration and silicification being predominant (Evans, 1993). Hyperspectral investigations of porphyry molybdenum deposits include those of Tukiainen and Thomassen (2010) and Bedini (2012) of the Climax-like Malmbjerg deposit in East Greenland.

The large size of the alteration system has also made the porphyry copper deposits a target of spaceborne hyperspectral remote sensing applications

using Hyperion EO-1 data (e.g. Zadeh et al., 2014). The hyperspectral imagery from spaceborne hyperspectral systems despite the moderate spatial resolution (30 m) has the potential to be successfully applied to characterize and detect alteration systems related with porphyry deposits.

The use of the hyperspectral thermal infrared imagery for the study of the surface exposures of porphyry deposits provides important information. Riley et al. (2009) used airborne hyperspectral thermal infrared data recorded by SEBASS imaging system to map the mineralogy of porphyry alteration zones (potassic, phyllic, argillic, and propylitic) at Yerington, Nevada. In addition, to the alteration minerals that can also be mapped using hyperspectral reflectance data (e.g., biotite, muscovite, gypsum, kaolinite, epidote, chlorite, etc.) the hyperspectral thermal infrared data mapped quartz, orthoclase, albite, pyrite (Riley et al., 2009).

Several studies have mapped alteration zones similar for porphyry deposits, although no deposits have been located in the respective study area. For example, Kruse (1988) has detected alteration systems characteristic for porphyry copper deposits in Northern Grapevine Mountains. Tukiainen and Thomassen (2010) report finding similar alteration features to the Malmbjerg porphyry molybdenum deposit some two km-south of the deposit. Bedini (2011) studied with airborne HyMap hyperspectral imagery an extensive hydrothermal alteration system at Kap Simpson in East Greenland. Based also on geochemical indicators it is believed that the alteration assemblage at Kap Simpson could be part of a porphyry molybdenum system. Ngcofe et al. (2013) mapped indicator alteration minerals for porphyry copper deposits in the Namaqua Metamorphic Province, South Africa, using HyMap imagery.

Epithermal high- and low-sulfidation gold-silver deposits

Epithermal deposits are low-temperature (< 300 °C), precious- or base-metal deposits with close temporal and spatial association with volcanic centres. Precious metals (Au and Ag) are the major products of epithermal deposits, although some produce by-product Hg and Sb, and by- or coproduct base metals Pb, Cu and Zn (Ridley, 2013). As epithermal deposits are formed at shallow depths (< 2 km), many probably become eroded relatively rapidly after formation. The majority of known deposits are thus geologically recent (Cenozoic), and occur in areas of active or recent arc volcanism. Detailed descriptions and numerous

references for the epithermal gold-silver deposits are given in Pirajno (2009).

The high-sulfidation epithermal gold deposits (or quartz-alunite epithermal gold deposits) show strong hydrothermal alteration of the wall-rock, often with well-defined zoning. The sulphates and clay-minerals (e.g., alunite, dickite, kaolinite, pyrophyllite, illite) that occur in the hydrothermal alteration zones (advanced argillic, intermediate argillic, and propylitic) of high-sulfidation epithermal gold deposits have unique spectral reflectance features in the short wave infrared wavelength region (e.g. Clark, 1999).

The hydrothermal alteration system of quartz-alunite epithermal gold deposits has been the target of numerous hyperspectral remote sensing studies (e.g. Goetz and Srivastava, 1985; Kruse et al., 1990; Clark et al., 2003; Kruse et al., 2003; Kruse et al., 2006; Bedini et al., 2009; Riley and Hecker, 2013; Swayze et al., 2014; among others). Goetz and Srivastava (1985) used data from the first hyperspectral sensor Airborne Imaging Spectrometer (AIS) to map kaolinite and alunite at Cuprite (Nevada) epithermal high-sulfidation alteration system. This study also detected from the AIS data, for the first time at Cuprite, the presence of the mineral buddingtonite, an ammonium-bearing feldspar (Goetz and Srivastava, 1985).

Kruse et al. (1990) using GERIS airborne hyperspectral data at Cuprite, mapped alunite, kaolinite, buddingtonite and hematite. Alunite, kaolinite, pyrophyllite, buddingtonite, muscovite, goethite, hematite etc., were mapped at Cuprite epithermal high-sulfidation alteration system by Clark et al. (2003) using AVIRIS hyperspectral data. Another detailed hyperspectral mapping of the alteration mineralogy at Cuprite is given in Swayze et al. (2014). Bedini et al. (2009) investigated using HyMap airborne hyperspectral imagery the extensive epithermal high-sulfidation hydrothermal alteration system associated with the Rodalquilar epithermal alunite gold deposits in southeast Spain. The HyMap mapping results for alunite, pyrophyllite, kaolinite and illite can be used to refine the map of the hydrothermal alteration zones at Rodalquilar (Bedini et al., 2009). Kruse et al. (2006) analyzed AVIRIS hyperspectral data at Los Menucos, Argentina. The alteration minerals identified in the Los Menucos district using the AVIRIS imagery include hematite, goethite, kaolinite, dickite, alunite, pyrophyllite, muscovite/sericite, montmorillonite, calcite, and zeolites (Kruse et al., 2006). The hyperspectral maps showed good correspondence with the results of field reconnaissance verification and spectral measurements acquired using a field spectrometer (Kruse et al., 2006).

The low-sulfidation epithermal gold-silver deposits have a weaker hydrothermal alteration of the wall-rock than the high-sulfidation epithermal gold-silver deposits. Crosta et al. (1998) carried out a study at Bodie, California, where a low-sulfidation epithermal gold deposit has been mined out (John et al., 2015). Bierwirth et al. (2002) analyzed HyMap hyperspectral data in the Indee district of the North Pilbara terrain in Western Australia, in an area where also occur epithermal-like vein gold deposits associated with quartz-mica alteration assemblage. They report that epithermal-like systems were characterized by Al-poor white mica and possibly tourmaline, minerals that were mapped from the hyperspectral data (Bierwirth et al., 2002).

The use of airborne thermal infrared hyperspectral imagery will open new insights to the study of the surface outcrops of epithermal gold and silver deposits, especially for the detection of quartz-rich zones (e.g. Vaughan et al., 2005; Calvin et al., 2015). Riley and Hecker (2013) used airborne hyperspectral thermal imagery to characterize the epithermal alteration system at Cuprite, Nevada. The airborne hyperspectral imagery mapped a series of minerals including quartz, alunite, kaolinite, muscovite, chlorite, orthoclase, oligoclase, sanidine (Riley and Hecker, 2013).

The hyperspectral mapping of active epithermal systems has given important information for the present-day epithermal systems (e.g. Kruse, 1999; Hellman and Ramsey, 2004; Kratt et al., 2010; van der Meer et al., 2014; Calvin et al., 2015). The use of the satellite hyperspectral imagery to characterize the alteration assemblage of the epithermal gold-silver deposits is more difficult due to the moderate spatial resolution of these data. However, some encouraging results have been reported (e.g. Kruse et al., 2003, 2006; Calvin and Pace, 2016).

The epithermal gold-silver deposits are well studied and represented in the geological hyperspectral literature. Simultaneous investigations of the alteration assemblages of such mineralizing systems using visible to short wave infrared and thermal infrared data will be very contributive.

Greisen and related ore deposits

The word greisen refers to a hydrothermal alteration assemblage of granitic rock, specifically quartz-muscovite (or lepidolite) with accessory amounts of topaz, tourmaline and fluorite formed by the post-magmatic metasomatic alteration of granite (e.g. Best, 1982). Greisens are important mainly for their production of tin and tungsten. They are usually

developed at the upper contacts of granite intrusions. The mineralization occurs as large irregular, or sheet-like bodies immediately beneath the upper contact of late stage, geochemically specialized granites and may extend downwards for some 10-100 m before grading through a zone of feldspathic alteration (albitization, microclinization) into fresh granite below (Pollard et al., 1988).

Muscovite, topaz and tourmaline have diagnostic absorption features in the SWIR wavelength region (e.g. Clark et al., 2003). These minerals can also be detected using hyperspectral data (e.g., Bierwirth et al., 2002; Bedini, 2012). There are few hyperspectral remote sensing studies of greisen related ore deposits. Tukiainen and Thomassen (2010) report that in Hudson Land in Greenland greisen mineralization that returned 1.4% Sn was not possible to be outlined from the hyperspectral data (5 m spatial resolution) due to the limited size of the outcrops.

More research using infrared spectroscopy and airborne hyperspectral imagery on the detection and mapping of greisen alteration products is needed.

Skarn deposits

A skarn deposit is an ore deposit in carbonate-bearing rocks that have been hydrothermally altered to assemblages of calc-silicate minerals together with, in some cases, magnetite or Mg-bearing gangue silicate minerals. The deposits are characteristically within about a kilometre distance of the contact of an igneous intrusion. Ore minerals occur in fractures or are disseminated through the altered rock (Ridley, 2013).

Zamuido (2009) targeted using airborne hyperspectral data gold-platinum mineralization occurring in skarns at the El Capitan iron deposit in New Mexico. The El Capitan deposit is characterized by iron-rich calc-silicate skarn mineralogy and a later stage hematite-calcite dominant assemblage. Gold-platinum mineralization occurs mainly in the hematite-calcite assemblage. The focus of the hyperspectral mineral mapping was on the carbonate rocks, calc-silicate skarn minerals (tremolite and phlogopite), hematite and goethite. Several anomalous areas of hematite/goethite and calc-silicates were identified. These anomalies were field checked and several were found to have anomalous gold and platinum values (Zamuido, 2009). The HyMap hyperspectral imagery was applied to the study of skarn-related Mary Kathleen metamorphic-hydrothermal U-REE deposit, NW, Queensland, Australia (Salles et al., 2017). The hyperspectral data were used to map the spatial distribution of scapolite, andradite, calcite, epidote, hornblende, montmorillonite, kaolinite and goethite.

The HyMap data offered comprehensive mineralogical examination between skarn assemblages and uneconomic host rock. The authors report also the detection by hyperspectral data of interesting patterns in the skarn alteration system and their relation with the ore deposit (Salles et al., 2017). Skarn-marble assemblages were also detected by spaceborne ASTER multispectral data (Rowan and Mars, 2003) indicating that for the remote sensing of skarns also satellite-based sensors could be useful.

Cudahy et al. (2000a) used airborne hyperspectral thermal infrared data to map skarn alteration mineralogy at Yerington, Nevada. The analysis of the thermal infrared hyperspectral imagery mapped Fe-garnet, Al-Fe garnet, pyroxene, epidote, dolomite, calcite, quartz-clay-feldspar, gypsum etc. In addition, the study aimed to distinguish garnet solid solution series. The map of the garnet Fe-Al solid solution chemistry clearly delineated those areas of skarn-alteration and was consistent with the skarn alteration zonation mapped by field geologists (Cudahy et al., 2000a). This study is not only important for the hyperspectral remote sensing of the skarn formations discussed in this subsection, but it shows the potential of well-analyzed hyperspectral thermal infrared data for mineral exploration. Kruse (2015) using hyperspectral thermal infrared data in a site in northern Death Valley, California and Nevada, also mapped calc-silicate alteration (andradite garnet skarn) and silicification. This alteration was the result of carbonate altered to skarn as verified by field observations (Kruse, 2015).

Volcanic-hosted massive sulfide (VHMS) deposits

Volcanic-hosted massive sulfide (VHMS) or volcanogenic massive sulfide (VMS) deposits are stratiform and sometimes stratiform bodies of massive sulfide hydrothermal ore and associated sulfidic ores (sulfidic sediments, disseminated replacement ores, stockwork sulfide-bearing veins) that formed at or just below the sea floor near active magmatic centres in relatively deep marine environments (Ridley, 2013).

The contribution of the hyperspectral remote sensing to the study of the VHMS deposits is mainly related with the detection of the minerals in the hydrothermal alteration assemblage. Knowledge on the alteration assemblage is important to understand the VHMS deposits (e.g. Franklin, 1993). In the VHMS deposits are generally distinguished silicic, chloritic, sericitic and carbonate alteration zones (Thompson and Thompson, 1996). The main alteration minerals that can be mapped from the hyperspectral data within these

alteration zones include sericite, chlorite, biotite, dolomite, calcite, etc. In addition, quartz can be mapped by hyperspectral thermal infrared data. Typically, the distribution of Fe and Mg-chlorite and sericite (muscovite) zones are used as a vector toward ore (Thompson et al., 1999). Several studies have investigated the spectral reflectance properties of alteration minerals associated with VHMS deposits. Herrmann et al. (2001) and Jones et al. (2005) used SWIR results from VHMS deposits in Tasmania–Queensland and Vancouver Island, British Columbia, respectively, to illustrate that subtle shifts in the white mica spectra (usually to lower wavelengths) can be used to define compositional change of the white micas which could be a potentially vector, toward some types of VHMS ore deposits.

The VHMS deposits have been in the focus of several hyperspectral remote sensing studies. Cudahy et al. (2000b) used airborne hyperspectral data to prospect for VHMS Zn mineralization at Panorama, Australia. HyMap airborne hyperspectral data were used to characterize VHMS deposits in Archaean greenstone belts in Australia by van Ruitenbeek et al. (2006, 2012). They focused on the change of the chemistry of the alteration mineral muscovite/sericite, which is associated with a change in the spectral reflectance feature of this mineral (e.g. Duke, 1994). Patterns of paleofluid flow in this VHMS alteration system were also found using hyperspectral data and subsequent field investigations (van Ruitenbeek et al., 2005). Laakso et al. (2015) investigated the VHMS Izok Lake Zn-Cu-Pb-Ag deposit, Nunavut in Canada, using field spectroscopy and airborne hyperspectral data. They report the finding of a phengite composition of the muscovite closer to the ore deposit. In addition, there was detected a change in the chemical composition of chlorite. In the Abitibi greenstone belt, Rivard et al. (2009) distinguished several lithologic units, among others rhyolites despite the extensive vegetation of the area. In this area the VHMS deposits are known to be associated with rhyolites (Rivard et al., 2009).

4.3 Hydrothermal ore deposits (orogenic environments)

Three important types of hydrothermal Au and Au–Cu deposits form during regional tectonism and within the time spans of active magmatism in the host geological terrains. These are: orogenic Au deposits, Carlin-type gold deposits and Iron oxide–copper–gold (IOCG) deposits (Ridley, 2013).

Orogenic Au deposits

Orogenic Au deposits are alternatively known as lode Au deposits, quartz vein Au deposits, Au-only deposits or mesothermal Au deposits. These are vein and replacement Au deposits in metamorphic and intrusive igneous rocks, most of which have formed broadly during periods of regional metamorphism.

Wang et al. (2017) investigated using infrared reflectance spectroscopy the alteration assemblage of two orogenic gold deposits in Australia (Sunrise Dam and Kanowna Belle). Both these gold deposits are structurally controlled and generated similar alteration mineral suites (largely white mica, chlorite, carbonate, quartz, pyrite ± epidote). Arne et al. (2016) studied by hyperspectral imaging selected drill cores from seven orogenic gold deposits in central Victoria, Australia. The most significant hyperspectral response lies in the white mica compositions, which vary in a systematic manner between high-Al muscovite zones (Al–OH absorption around 2208 nm) that define a phyllic alteration halo around mineralized structures, and low-Al phengitic–chlorite zones (Al–OH absorption >2014 nm) inferred to represent either more distal alteration or possibly regional metamorphic background (Arne et al., 2016). The Al content in the white mica (sericite) is indicated by the wavelength position of the Al–OH absorption feature (Duke 1994).

Bierwirth et al. (2002) investigated the outcropping alteration mineralogy of orogenic gold deposits in Indee district, Central Pilbara, Western Australia using airborne HyMap hyperspectral imagery. The analysis of the hyperspectral data mapped white mica, pyrophyllite, Fe-chlorite, kaolinite, goethite, hematite in the zones where the known lode gold deposits occur. As one type of these gold deposits is associated with pyrophyllite-bearing alteration, the detection of new pyrophyllite occurrences from the hyperspectral data represented possible new prospects (Bierwirth et al., 2002). In addition, high-Al white mica was observed to be associated with the lode Au deposits.

Carlin-type gold deposits

Carlin-type gold deposits are named after the type locality in Nevada, USA. Based on the host-rocks and the nature of the ore, they have been alternatively named sediment-hosted gold deposits and disseminated gold deposits. Carlin-type ore is characterized by disseminated, Au-bearing, and trace element-rich pyrite that occurs in replacement bodies in carbonate host rocks (Cline et al., 2005). Host rocks are typically decarbonatized, argillized, and variably silicified in addition to being sulfidized and enriched with Au. As the reactions that formed Au-bearing pyrite are

generally not the same reactions that formed alteration minerals (Hofstra et al., 1991), ore and alteration zoning within the deposits is irregular. This lack of a temporal, and thus spatial relationship, along with the fine grained nature and sparse abundance of ore and alteration minerals, limits the use of alteration to identify ore (Cline et al., 2005).

Studies using X-ray diffraction (XRD) analysis have shown that illite in the argillized alteration zones of the Carlin-type gold deposits ranges from well-ordered high temperature 2M to poor-ordered low temperature 1M variety (Kruse and Hauff, 1991). Kruse and Hauff (1991) in a study at Carlin gold mine in Eureka County, Nevada, have shown that these illite polytype zoning can be distinguished also by short-wave infrared spectroscopy techniques. Similar polytype zoning within the argillized alteration zone have also been evidenced for kaolinite and dickite alteration minerals (Cline et al., 2005). These features in the alteration zone could be identified using SWIR-techniques and mapped by hyperspectral image analysis.

Ammoniated hydrothermal fluids interact with potassium-bearing minerals in wall rock material to form ammonium illite alteration patterns along fluid conduits associated with Carlin-type gold deposits. These same fluids transport gold which is disseminated into favorable host rock. Thus, ammonium illite serves as an exploration tool for locating Carlin-type gold deposits. Ammonium illite was mapped using HyMap hyperspectral data at the Waterpipe Canyon area (Jerritt Canyon district) and at the North Screamer deposit, Nevada, USA (Mateer, 2010). In addition, Mateer (2010) observed that phengitic illite that can be mapped from the hyperspectral data, is an indicator of hydrothermal activity and can be a useful guide for Carlin-type gold exploration at these localities.

Another characteristic of the Carlin-type gold deposits that is observed in many cases is the silicification. Multispectral airborne and spaceborne thermal infrared data have been applied to identify silica-rich zones as an indicator of probable mineralization processes (Watson et al., 1990; Rockwell and Hofstra, 2008). This indicates that more detailed airborne hyperspectral thermal infrared data will be useful for the exploration of Carlin-type gold deposits. Spaceborne hyperspectral Hyperion EO-1 data have been evaluated for the detection of iron oxides/hydroxides and clay-rich zones associated with the known Carlin-style gold deposits in the Bau district, Malaysia. The authors report encouraging results despite the moderate spatial resolution of the

spaceborne hyperspectral data (Pour and Hashim, 2014).

Iron oxide–copper–gold (IOCG) deposits

Iron oxide–copper–gold (IOCG) deposits are hydrothermal ores most importantly of copper and gold, but which may also produce other metals as by- and co-products (U, Ag, LREEs). The distinct characteristic of these deposits is that the major Fe-bearing mineral in ore is magnetite or hematite rather than an iron sulfide mineral such as pyrite (Ridley, 2013).

Corriveau et al. (2007) evaluating the useful techniques for the prospection of IOCG deposits in volcano-plutonic terrains of Canada using alteration as a vector to ore, also discuss the hyperspectral signatures of alteration zones associated with IOCG deposits. The potassic and sodic alteration show similar overall profiles but can be distinguished on the basis of the location of hydroxyl feature (OH-) near 2200nm. These results suggest a potential to remotely map the distribution of these alteration types using hyperspectral airborne or spaceborne imaging given sufficient spatial resolution (Corriveau et al., 2007). Near infrared reflectance spectroscopy was used to investigate the composition of phengite alteration mineral at the Olympic Dam IOCG deposit (Tappert et al., 2013). The study reports that phengite located near the ore-bearing zone was found to contain more aluminum than phengite located in the barren rocks, and this difference in phengite mineral chemistry was observable in the reflectance spectra between 2.206 μm and 2.213 μm .

Airborne hyperspectral images from the Eastern Fold Belt of the Mount Isa Inlier, Australia were tested for the detection of Fe-oxide Cu–Au (IOCG) related alteration by Laukamp et al. (2011). Different types of hydrothermal alteration and paleofluid channels were identified by mapping the spatial distribution, degree of crystallinity and the composition of alteration minerals (white micas, amphibole, chlorite, etc.).

4.4 Hydrothermal ore deposits (sedimentary environments)

In this group are included Mississippi Valley-type (MVT) Pb-Zn deposits and SEDEX Pb-Zn-Ag deposits, Kupferschiefer or red-bed copper deposits and Uranium deposits in sedimentary basins (Evans, 1993). Mississippi Valley-type deposits are epigenetic Pb–Zn sulfide deposits in carbonate rocks which contain a few per cent to up to about 10 wt % of each of Pb and Zn, with approximately equal grades of the

two or dominated by Zn. Kupferschiefer deposits are generally large, laterally extensive, stratabound Cu deposits, with Co as an important by-product in some deposits. The majority of uranium resources are ores formed by syn-diagenetic migration of low temperature waters through sedimentary basins, in particular through high-permeability sandstones in intracontinental basins (Ridley, 2013). The geological hyperspectral remote sensing literature is poor in the study of the Mississippi Valley-type (MVT) Pb-Zn deposits, Kupferschiefer deposits and uranium deposits in sedimentary basins.

SEDEX Pb-Zn-Ag deposits

SEDEX deposits are in some respects similar to MVT ores. They are stratiform or stratabound Pb-Zn sulfide ores hosted in sedimentary rock of early-Proterozoic to Mesozoic age, with Ag as a significant co-product in many ores and in some cases minor Cu (e.g. Ridley, 2013). Peter et al. (2015) carried out a VNIR-SWIR spectroscopy study of the sediment-hosted Zn-Pb deposits (SEDEX) in basinal shale environments of the Howard's Pass and MacMillan Pass districts, Selwyn Basin, Canada. Many of the key minerals spatially associated with sediment-hosted Zn-Pb mineralization in the Selwyn Basin (apatite, pyrite, sphalerite, barite, K-Ba feldspar) do not have spectral signatures in the VNIR-SWIR portion of the electromagnetic spectrum. However, the data indicated that other minerals that are spatially associated with mineralization (siderite, muscovite, phengite, and montmorillonite) do have spectral signatures, although they are quite muted (Peter et al., 2015). They conclude that hyperspectral optical reflectance spectroscopy will be of limited use in delineating favorable horizons and vectoring toward mineralization along them in Howard's Pass and MacMillan Pass districts of the Selwyn Basin (Peter et al., 2015).

Cudahy et al. (1999) mapped garnet Fe-Mn solid solution chemistry associated with Broken Hill style Pb-Zn-Ag mineralization using airborne hyperspectral 9-11 μm data. It was observed that garnet composition becomes Mn-rich (spessartine) near stratabound Pb-Zn-Ag mineralization. Most authors consider the Broken Hill-type Pb-Zn-Ag deposits to be a metamorphosed variant of the SEDEX deposits (Walters, 1998). Abundant sillimanite and disseminated garnet form large-scale stratabound alteration envelopes in host quartzo-feldspathic sequences. Fe-Mn garnet quartzites and sandstones form immediate envelope to ore system (Walters, 1998). Airborne HyMap hyperspectral data have also been used at Broken Hill (Taylor et al., 2005). HyMap

data were able to map certain lithologies critical to mineral exploration in the region, such as gahnite-bearing quartz, manganese-bearing garnetiferous rocks, and sodium-rich micas indicative of likely mineral alteration. Pb-Zn-Ag-deposits at Mount Isa, Australia were also targeted by HyMap hyperspectral data (Jakob et al., 2016). The authors focused mainly at the detection of gossans that can be related with the mineralization.

4.5. Ore deposits formed in sedimentary environments

In this group are included iron ores in banded-iron formations and sedimentary-rock hosted Mn deposits. The banded-iron formations occur in stratigraphical units hundreds of meters thick and hundreds or even thousands of kilometres in lateral extent. Substantial parts of these iron formations are usable directly as a low grade iron ore (e.g. taconite) and other parts have been the protores for higher grade deposits (Evans, 1993). The majority of Mn supply and the majority of known Mn resources are from a small number of large, stratiform deposits of late-Archaeon to Tertiary age hosted in sequences of shallow marine sedimentary rocks that formed distant from active volcanism. By analogy with iron formations, these are sometimes known as manganese formations (Ridley, 2013). An application of spaceborne ASTER multispectral data to target iron ore in banded iron formations at Weld Range Greenstone Belt, Yilgarn Craton, Western Australia (Duuring et al., 2012) indicates the potential of remote sensing data to characterize banded-iron formations and related deposits.

Case studies of the application of airborne and spaceborne hyperspectral remote sensing to characterize these deposits (iron ores in banded-iron formations and sedimentary-rock hosted Mn deposits) will be valuable to the geological remote sensing literature.

4.6 Supergene ores

Laterites and bauxites

Supergene implies genesis at or near the Earth's surface. The word is used to contrast with hypogene, or genesis at depth. In most cases, supergene ores are formed as a result of action of meteoric waters on rocks through the chemical processes and mineral reactions of weathering (e.g. Evans, 1993; Ridley, 2013). The term 'laterite' refers to red-coloured iron oxide- and alumina-rich subsoil that is leached of bases and is characteristic of weathering of essentially all rock types in climatic zones of intense chemical

weathering. Bauxites are regolith materials composed of mixtures of fine-grained aluminum hydroxide minerals, most commonly the hydrated mineral gibbsite ($\text{Al}_2\text{O}_3 \cdot 3\text{H}_2\text{O}$) and semihydrated boehmite ($\text{AlO} \cdot \text{OH}$), or more rarely diasporite ($\text{AlO} \cdot \text{OH}$). Most bauxites include both gibbsite and boehmite, although one of the two is generally dominant. Bauxite ores in lateritic regolith profiles contribute almost all of the world's Al resources (Ridley, 2013).

Carvalho et al. (1999) report the evaluation of AVIRIS hyperspectral data to study the supergene nickel laterite accumulations near the Niquelandia town, Goiás State, Brazil. The nickel laterite deposit of Niquelandia is the product of the weathering of an ultramafic-alkaline massif. There are distinguished two types of ore: garnierite and limonitic ore. The authors report the mapping of the principal weathering horizon profiles from the hyperspectral data. Garnierite, kaolinite, iron oxides and hydroxides were distinguished by AVIRIS data analysis (Carvalho et al., 1999). Nagal (2013) used spaceborne Hyperion-EO1 hyperspectral data to detect bauxite accumulations in a part of Katni District, Madhya Pradesh, India. Conventional techniques to demarcate the high-grade pockets of bauxites rich in gibbsite are tedious, time consuming and involve detailed field sampling and geochemical analyses. Kusuma et al. (2012) in a case study from the Savitri River Basin, Maharashtra, India, show how spectral properties can be effectively utilized in mapping of high-grade bauxites occurring over wide areas using spaceborne hyperspectral remote sensing data (Hyperion EO-1).

5. Discussion

The previous section presented a systematic, up-to-date and almost exhaustive review of the literature on the applications of hyperspectral remote sensing to mineral exploration and ore deposit characterization. Based on this review this section discusses some of the key aspects of hyperspectral imaging for mineral exploration and ore deposit characterization.

Not all types of ore deposits have had the same attention from the geological hyperspectral research community (Table 1). Particularly investigated by hyperspectral imaging are the epithermal gold deposits and to some extent the porphyry copper deposits. Several studies have also been reported for kimberlites (host-rock of diamonds), carbonatites (host-rock of rare earth elements), skarn deposits, VHMS deposits, orogenic hydrothermal ore deposits and SEDEX Pb-

Zn-Ag deposits. Underexplored is the possibility of hyperspectral imaging for the characterization of a number of ore deposits including chromites and nickel-sulfides in mafic and ultramafic rocks, rare-metal pegmatites, and supergene ores (laterites and bauxites). On the other hand, for a number of ore deposits related with the sedimentary environments including Mississippi Valley-type (MVT) Pb-Zn deposits, Kupferschiefer deposits and uranium deposits in sedimentary basins, iron ores in banded-iron formations have not been reported hyperspectral imaging studies.

The limited or missing hyperspectral case studies for a number of important ore deposits is related at least with two factors: (1) the still limited availability of airborne hyperspectral imagery to the research community; (2) the efficacy of the hyperspectral imaging for the characterization of a given deposit. However, as mentioned in several cases in Section 3, for a number of these deposits infrared spectroscopy and close-range spectral imaging techniques have indicated that the airborne and spaceborne hyperspectral remote sensing can make a contribution for their exploration.

Hyperspectral case studies showing the possibilities of the technology for the exploration and characterization of these ore deposit types for which the use of the hyperspectral technology is still underexplored would be very contributive to the geological remote sensing literature.

The hyperspectral data analysis and interpretation can target directly the ore mineralization, the hydrothermal alteration associated with the ore mineralization, or the host-rock of the mineralization. The review of the literature (Table 1) shows that in the exploration and characterization of an ore deposit the focus of the hyperspectral data analysis can vary based on the (1) type of mineral deposit; (2) wavelength of the hyperspectral imagery available and (3) degree of surface exposure.

Characteristically, the hyperspectral investigation of magmatic ore deposits is usually based on the detection of the host-rock. Generally, in all types of hydrothermal ore deposits, the hyperspectral image analysis focuses on the mapping of the alteration minerals in the various alteration assemblages associating these ore deposits. The direct detection of ore minerals is less common. Examples could be the attempt to directly detect absorption features of rare earth elements in carbonatites or the mapping of iron oxides/hydroxides and garnierite in iron-nickel laterites.

Table 1. Major ore deposit types, quantity of reported hyperspectral imaging studies of these deposits, and the main focus of the hyperspectral data analysis.

	Ore deposit	Hyperspectral imaging studies reported in the literature	Focus of hyperspectral data analysis
Magmatic	Diamonds in kimberlites	several studies	host-rock
	Rare earth elements in carbonatites	several studies	host-rock; mineral alteration; ore minerals
	Chromite deposits in mafic and ultramafic rocks	limited number of studies	host-rock
	Nickel sulfide deposits in mafic and ultramafic rocks	limited number of studies	host-rock
	Rare-metal pegmatites	limited number of studies	host-rock
Hydrothermal ore deposits (magmatic environments)	Porphyry copper and porphyry molybdenum deposits	a large number of studies	alteration minerals
	Epithermal gold-silver deposits	a large number of studies	alteration minerals
	Greisen-related ore deposits	no studies reported	
	Skarn deposits	several studies	host-rock; alteration minerals
	Volcanic-hosted massive sulfide (VHMS) deposits	several studies	alteration minerals
Hydrothermal ore deposits (orogenic environments)	Orogenic Au deposits	several studies	alteration minerals
	Carlin-type gold deposits	several studies	host-rock; alteration minerals
	Iron oxide–copper–gold (IOCG) deposits	several studies	alteration minerals
Hydrothermal ore deposits (sedimentary environments)	SEDEX Pb-Zn-Ag deposits	several studies	alteration minerals
	Mississippi Valley-type (MVT) Pb-Zn deposits	no studies reported	
	Kupferschiefer copper deposits	no studies reported	
	Uranium deposits in sedimentary basins	no studies reported	
Ore deposits formed in sedimentary environments	Banded-iron formations and sedimentary-rock hosted Mn deposits, etc.	no studies reported	
Supergene ores	Laterites and bauxites	limited number of studies	host-rock, ore minerals

The spectral resolution of the airborne hyperspectral systems in the studies considered in this review is generally not reported as problematic for the detection of the targeted minerals or host-rock lithology. This implies that a spectral resolution of 10 to 20 nm (AVIRIS and HyMap sensors) achieves the goals of a mineral mapping application including the specific detection of solid solution series reflected in the shifting of absorption features (e.g. the Al-OH absorption feature of micas around 2.2 μm). An exception is related with the objective of the direct detection of rare earth element absorption features. In this case the spectral resolution in the VNIR wavelength region may not satisfy the requirements for the REE detection.

The spatial resolution is another key aspect of a geological remote sensing application. A number of studies listed in the review could not achieve their objective due to the low spatial resolution of the hyperspectral imagery in relation to the surface outcrop of the targeted mineral or lithology. In general, for all the applications a higher spatial resolution would be beneficial for a more detailed mapping and detection of the outcropping minerals and rock units. In some studies (e.g. Kruse and Boardmann, 2000), hyperspectral data of various spatial resolution have been acquired for the same target area.

To be mentioned that a higher spatial resolution is associated with a smaller area imaged across the track. This increases the number of flight lines needed to cover a given area and with it also increases the computational task for the hyperspectral image analyst. The simultaneous processing of such data consisting of numerous flight lines is often hindered from calibration problems, varying weather conditions, BRDF effects etc. In this respect, the acquisition of hyperspectral data of high spatial resolution and with a large swath would be a much appreciated technological advancement.

The overwhelming majority of airborne hyperspectral remote sensing mineral exploration studies reported in the literature are carried out in U.S.A and Australia, and to a less extent in Canada, Greenland, Argentina, Brasil, Spain, Namibia etc. The availability to interested researchers (especially in the developing countries) of good quality airborne hyperspectral data is still very limited. Problems with noise and area coverage hinder the routine application of data from the Hyperion EO-1 sensor, the only source of free available spaceborne hyperspectral data to-date. Data from several national spaceborne hyperspectral sensors are only available (or will be only available) to national institutions and not to the broad research

community. In this situation, the only perspective for good quality spaceborne hyperspectral data to the broad hyperspectral research community is the planned NASA's HySpIRI mission (e.g. Lee et al., 2015).

6. Concluding remarks

This article reviewed the use of hyperspectral remote sensing for mineral exploration. The main ore deposit types were grouped following a schema generally based on major processes of formation (magmatic, hydrothermal, sedimentary, supergene) and host-rock type. The review shows that the hyperspectral remote sensing technology has found application to the study and exploration of numerous ore deposits including detection of kimberlites (host-rocks of diamonds), carbonatites (host-rock of rare earth elements deposits), porphyry deposits, epithermal gold and silver deposits, skarn deposits, volcanic-hosted massive sulfide (VHMS) deposits, orogenic gold deposits, Carlin-type gold deposits, Iron oxide-copper-gold (IOCG) deposits, SEDEX Pb-Zn-Ag deposits. However, the possibilities of the hyperspectral technology remain still underexplored for the study and exploration of chromite deposits, Ni-sulfide deposits in mafic and ultramafic rocks, rare-metal pegmatites, greisen and related deposits, Mississippi Valley-type (MVT) Pb-Zn deposits, Kupferschiefer deposits and uranium deposits in sedimentary basins, iron ores in banded-iron formations, sedimentary-rock hosted Mn deposits, laterites and bauxites. Indeed, in many cases, studies using infrared spectroscopy techniques have indicated the possibility of the application of hyperspectral remote sensing to the characterization of these deposits.

The increased availability to the interested researchers and exploration companies of airborne and spaceborne hyperspectral imagery will make possible case studies on the hyperspectral characterization of these deposit types which up to now have limited or no applications of hyperspectral remote sensing. The use of hyperspectral thermal infrared imagery has the potential to open new perspectives on the hyperspectral remote sensing of the Earth's resources. In addition, more refinements and mapping techniques and strategies have to be developed to increase the impact of the hyperspectral technology in the mineral exploration industry.

References

- Arne, D., House, E., Pontual, S., Huntington, J., 2016. Hyperspectral interpretation of selected drill cores

- from orogenic gold deposits in central Victoria, Australia. *Australian Journal of Earth Sciences* 63, 1003–1025.
- Asadzadeh, S., Souza, C.R.de, 2016. A review on spectral processing methods for geological remote sensing. *International Journal of Applied Earth Observation and Geoinformation* 47, 69–90.
- Baldrige, A.M., Hook, S.J., Grove, C.I., Rivera, G., 2009. The ASTER spectral library version 2.0. *Remote Sensing of Environment* 113, 711–715.
- Bedell, R., 2004. Remote sensing in mineral exploration. *Society of Economic Geologists, SEG Newsletter* 58, 8–14.
- Bedini, E., Rasmussen, T.M., 2017. Use of airborne hyperspectral imagery and gamma-ray spectroscopy data for mineral exploration at the Sarfartoq carbonatite complex, southern West Greenland. *Geoscience Journal (submitted)*.
- Bedini, E., 2012. Mapping alteration minerals at Malmbjerg molybdenum deposit, East Greenland, by Kohonen self-organizing maps and matched filter analysis of hyperspectral imagery. *International Journal of Remote Sensing* 33, 939–961.
- Bedini, E., 2011. Mineral mapping in the Kap Simpson complex, central East Greenland using HyMap and ASTER remote sensing data. *Advances in Space Research* 47, 60–73.
- Bedini, E., 2009. Mapping lithology of the Sarfartoq carbonatite complex, southern West Greenland, using HyMap imaging spectrometer data. *Remote Sensing of Environment* 113, 1208–1219.
- Bedini, E., van der Meer, F., van Ruitenbeek, F., 2009. Use of HyMap imaging spectrometer data to map mineralogy in the Rodalquilar caldera, southeast Spain. *International Journal of Remote Sensing* 30, 327–348.
- Berger, B.R., King, T.V.V., Morath, L.C., Phillips, J.D., 2003. Utility of high-altitude infrared spectral data in mineral exploration: application to northern Patagonia Mountains, Arizona. *Economic Geology* 98, 1003–1018.
- Best, M.C., 1982. *Igneous and Metamorphic Petrology*. Freeman, San Francisco.
- Bierwirth, P., Huston, D., Blewett, R., 2002. Hyperspectral mapping of mineral assemblages associated with gold mineralization in the Central Pilbara, Western Australia. *Economic Geology* 97, 819–826.
- Boesche, N., Rogass, C., Lubitz, C., Brell, M., Herrmann, S., Mielke, C., Tonn, S., Appelt, O., Altenberger, U., Kaufmann, H., 2015. Hyperspectral REE (rare earth element) mapping of outcrops applications for neodymium detection. *Remote Sensing* 7, 5160–5186.
- Calvin, W.M., Pace, E.L., 2016. Utilizing HypSIRI prototype data for geological exploration applications: a southern California case study. *Geosciences* 6, 11.
- Calvin, W.M., Littlefield, E.F., Kratt, C., 2015. Remote sensing of geothermal-related minerals for resource exploration in Nevada. *Geothermics* 53, 517–526.
- Carvalho, O.A.de, Martins, E.deS., Baptista, G.M. deM., Carvalho A.F.de, Madeira Netto, J.daS., Meneses, P.R., 1999. Mineralogical Differentiation in Weathering Profiles of Lateritic Ni Using AVIRIS Data in Niquelandia - GO, Brazil. 9th Airborne Visible/Infrared Imaging Spectrometer (AVIRIS) Workshop.
- Clark, R.N., Swayze, G.A., Wise, R., Livo, E., Hoefen, T., Kokaly, R., Sutley, S.J., 2007. USGS digital spectral library splib06a. U.S. Geological Survey, Digital Data Series 231.
- Clark R.N., Swayze G.A., Livo, K.E, Kokaly, R.F, Sutley, S.J, Dalton, J.B, McDougal, R.R, Gent, C.A., 2003. Imaging spectroscopy: Earth and planetary remote sensing with the USGS Tetracorder and expert systems. *Journal Geophysical Research-Planets* 108, 44.
- Clark, R.N., 1999. Spectroscopy of rocks and minerals, and principles of spectroscopy, in: Rencz, A.N. (ed.), *Remote Sensing for the Earth Sciences*, v. 3. John Wiley, New York, pp. 3–58.
- Clénet, H., Ceulenee, G., Pinet, P., Abily, B., Daydou, Y., Harris, E., Dantas, C., 2010. Thick sections of layered ultramafic cumulates in the Oman ophiolite revealed by an airborne hyperspectral survey: petrogenesis and relationship to mantle diapirism. *Lithos* 114, 265–281.
- Cline, J.S., Hofstra, A.H., Muntean, J.L., Tosdal, R.M., Hickey, K.A., 2005. Carlin-type gold deposits in Nevada: Critical geological characteristics and viable models. *Economic Geology* 100, 451–484.
- Cloutis, E.A., Sunshine, J.M., Morris, R.V., 2004. Spectral reflectance-compositional properties of spinels and chromites: Implications for planetary remote sensing and geothermometry. *Meteoritics and Planetary Science* 39, 545–565.
- Cloutis, E.A., 1996. Hyperspectral geological remote sensing: Evaluation of analytical techniques. *International Journal of Remote Sensing* 17, 2215–2242.
- Christensen, P.R., Bandfield, J.L., Hamilton, V.E., Howard, D.A., Lane, M.D., Piatek, J.L., Ruff, S.W., Stefanov, W.L., 2000. A thermal emission spectral library of rock-forming minerals. *Journal*

- of Geophysical Research (Planets) E4 105, 9735–9739.
- Cocks, T., Jensen, R., Stewart, W.I., Shields, T., 1998. The HyMap airborne hyperspectral sensor: the system, calibration and performance. 1st EARSeL Workshop on Imaging Spectroscopy.
- Corriveau, L., Ootes, L., Mumin, H., Jackson, V., Bennett, V., Cremer, J.F., Rivard, B., McMartin, I., Beaudoin, G., 2007. Alteration vectoring to IOCG(U) deposits in frontier volcano-plutonic terrains, Canada. 5th International Conference on Mineral Exploration.
- Coulter, D.W., Hauff, P.L., Sares, M.A., Bird, D.A., Peters, D.C., Henderson, F.B., 2009. Hyperspectral remote sensing of a mineralized system in the Grizzly Peak caldera, Colorado: implications for exploration and acid drainage baselines. *Reviews in Economic Geology* 16, 123–134.
- Crosta, A.P., Sabine, C., Taranik, J.V., 1998. Hydrothermal alteration mapping at Bodie, California, using AVIRIS hyperspectral data. *Remote Sensing of Environment* 65, 309–319.
- Cudahy, T.J., 2016. Mineral mapping for exploration: an Australian journey of evolving spectral sensing technologies and industry collaboration. *Geosciences* 6, 52.
- Cudahy, T.J., Okada, K., Yamato, Y., Huntington, J.F., Hackwell, J.A., 2000a. Mapping skarn alteration mineralogy at Yerington, Nevada, using airborne hyperspectral TIR SEBASS imaging data. 14th International Conference on Applied Geologic Remote Sensing.
- Cudahy, T.J., Okada, K., Brauhart, C., 2000b. Targeting VMS-style Zn mineralisation at Panorama, Australia, using airborne hyperspectral VNIR-SWIR HYMAP™ data. 14th International Conference on Applied Geologic Remote Sensing.
- Cudahy, T.J., Okada, K., Whitbourn, L.B., 1999. Mapping garnet Fe-Mn solid solution chemistry associated with Broken Hill style Pb-Zn-Ag mineralisation using airborne hyperspectral 9-11 m reflectance. 13th ERIM International Conference on Applied Geologic Remote Sensing.
- Duke, E.F., 1994. Near-infrared spectra of muscovite, Tschermak substitution, and metamorphic reaction progress—implications for remote-sensing. *Geology* 22, 621–624.
- Duuring, P., Hagemann, S.G., Novikova, Y., Cudahy, T., Laukamp, C., 2012. Targeting iron ore in banded iron formations using ASTER data: Weld Range Greenstone Belt, Yilgarn Craton, Western Australia. *Economic Geology* 107, 585–597.
- Eisman, M.T., 2012. *Hyperspectral Remote Sensing*. SPIE Press, Bellingham.
- Evans, A.M., 1993. *Ore Geology and Industrial Minerals*, Third Edition. Blackwell Publishing.
- Franklin, J.M., 1993. Volcanic-associated massive sulfide deposits, in: Kirkham, R.V., (Ed.), *Mineral Deposit Modeling: Geological Association of Canada Special Paper* 40, 403–417.
- Goetz, A.F.H., Srivastavam V., 1985. Mineralogical mapping in the Cuprite mining district, Nevada. *Proceedings of the Airborne Imaging Spectrometer Data Analysis Workshop*. JPL Publication, Pasadena.
- Goetz, A.F.H., Vane, G., Solomon, J., Rock, B.N., 1985. Imaging spectrometry for Earth remote sensing. *Science* 228, 1147–1153.
- Goetz, A.F.H., 2009. Three decades of hyperspectral remote sensing of the Earth: a personal view. *Remote Sensing of Environment* 113, S5–S16.
- Green, R.O., Eastwood, M.L., Sarture, C.M., Chrien, T.G., Aronsson, M., Chippendale, B.J., Faust, J.A., Pavri, B.E., Chovit, C.J., Solis, M., 1998. Imaging spectroscopy and the Airborne Visible Infrared Imaging Spectrometer (AVIRIS). *Remote Sensing of Environment* 65, 227–248.
- Guha, A., Ravi, S., Ananth Rao, D., Vinod Kumar, K., Dhananjaya Rao, E.N., 2013. Issues and limitations of broad band remote Sensing of kimberlite—a case example from kimberlites of Dharwar Craton, India. *International Journal of Geosciences* 4, 371–379.
- Hauff, P.L., 2009. Alteration mineralogy of Alberta kimberlites: PIMA infrared spectroscopic analysis. *Alberta Geological Survey Special Report* 12, 79.
- Hellman, M.J., Ramsey, M.S., 2004. Analysis of hot springs and associated deposits in Yellowstone National Park using ASTER and AVIRIS remote sensing. *Journal of Volcanology and Geothermal Research* 135, 195–219.
- Herrmann, W., Blake, M., Doyle, M., Huston, D., Kamprad, J., Merry, N., Pontual, S., 2001. Short wavelength infrared (SWIR) spectral analysis of hydrothermal alteration zones associated with base metal sulphide deposits at Rosebery and Western Tharsis, Tasmania, and Highway-Reward, Queensland. *Economic Geology* 96, 939–955.
- Hunt, G.R., 1982. Spectroscopic properties of rocks and minerals, in: Carmichael, R. S. (Ed.), *Handbook of Physical Properties of Rocks* CRC Press, pp. 295–385.
- Jakob, S., Gloaguen, R., Laukamp, C., 2016. Remote Sensing-Based Exploration of Structurally-Related Mineralizations around Mount Isa, Queensland, Australia. *Remote Sensing* 8, 358.

- John, D.A., du Bray, E.A., Henry, C.D., Vikre, P.G., 2015. Cenozoic Magmatism and Epithermal Gold-Silver Deposits of the Southern Ancestral Cascade Arc, Western Nevada and Eastern California.
- Jones, S., Herrmann, W., Gemmell, B., 2005. Short wavelength infrared spectral characteristics of the HW horizon: Implications for exploration in the Mira Falls volcanic-hosted massive sulphide camp, Vancouver Island, British Columbia, Canada. *Economic Geology* 100, 273–294.
- Keeling, J.L., Mauger, A.J., Raven, M.D., 2004. Airborne hyperspectral survey and kimberlite detection in the Terowie district, South Australia, in: Roach, I.C. (ed.), *Regolith*. CRC LEME, pp. 166–170.
- Kokaly, R.F., Johnson, M.R., 2011. Chapter 21B. Analysis of Imaging Spectrometer Data for the Khanneshin Area of Interest. 24 p. In: Peters, S.G., King, T.V.V., Mack, T.J., and Chornack, M.P., eds., and the U.S. Geological Survey Afghanistan Mineral Assessment Team, 2011, Summaries of important areas for mineral investment and production opportunities of nonfuel minerals in Afghanistan: U.S. Geological Survey Open-File Report 2011–1204.
- Kratt, C., Calvin, W.M., Coolbaugh, M.F., 2010. Mineral mapping in the Pyramid Lake basin: hydrothermal alteration, chemical precipitates and geothermal energy potential. *Remote Sensing of Environment* 114, 2297–2304.
- Kruse, F.A., 2015. Integrated visible and near infrared, shortwave infrared, and longwave infrared (VNIR-SWIR-LWIR), full-range hyperspectral data analysis for geologic mapping. *Journal of Applied Remote Sensing* 9, 20.
- Kruse, F.A., 2012, Mapping Surface Mineralogy Using Imaging Spectrometry. *Geomorphology* 137, 41–56.
- Kruse, F.A., Taranik, J.V., Coolbaugh, M., Michaels, J., Littlefield, E.F., Calvin, W.M., Martini, B.A., 2011. Effect of Reduced Spatial Resolution on Mineral Mapping Using Imaging Spectrometry – Examples Using HypSPIRI-Simulated Data. *Remote Sensing* 3, 1584–1602.
- Kruse, F.A., Perry, S.L., Caballero, A., 2006. District-level mineral survey using airborne hyperspectral data, Los Menucos, Argentina. *Annals of Geophysics* 49, 83–92.
- Kruse, F.A., Boardman, J.W., Huntington, J.F., 2003. Comparison of airborne hyperspectral data and EO-1 Hyperion for mineral mapping. *IEEE Transactions on Geoscience and Remote Sensing* 41, 1388–1400.
- Kruse, F.A., Boardman, J.W., 2000. Characterization and mapping of kimberlites and related diatremes using hyperspectral remote sensing. *IEEE Trans. Geosci. Remote Sensing* 3, 299–304.
- Kruse, F.A., 1999. Mapping hot spring deposits with AVIRIS at Steamboat Springs, Nevada, in: Green, R.O. (Ed.), 8th Annual JPL Airborne Earth Science Workshop. Jet Propulsion Laboratory, pp. 239–245
- Kruse, F.A., Hauff, P.L., 1991. Identification of illite polytype zoning in disseminated gold deposits using reflectance spectroscopy and X-ray diffraction – potential for mapping with imaging spectrometers. *IEEE Transactions on Geoscience and Remote Sensing* 29, 101–104.
- Kruse, F.A., Kierein-Young, K.S., Boardman, J.W., 1990. Mineral mapping at Cuprite, Nevada with a 63 channel imaging spectrometer. *Photogramm. Engineering and Remote Sensing* 56, 83–92.
- Kruse, F.A., 1988. Use of airborne imaging spectrometer data to map minerals associated with hydrothermally altered rocks in the northern Grapevine Mountains, Nevada and California. *Remote Sensing Environment* 24, 31–51.
- Kuosmanen, V., Arkimaa, H., Tiainen, M., Bäs, R., 2015. Hyperspectral close-range LWIR imaging spectrometry – 3 case studies. *Geophysical signatures of mineral deposit types in Finland* Edited by Meri-Liisa Airo, Geological Survey of Finland, Special Paper 58, 117–144.
- Kusuma, K.N., Ramakrishnan, D., Pandalai, H.S., 2012. Spectral pathways for effective delineation of high-grade bauxites: a case study from the Savitri River Basin, Maharashtra, India, using EO-1 Hyperion data. *International Journal of Remote Sensing* 33, 7273–7290.
- Laakso, K., Rivard, B., Peter, J.M., 2015. Hyperspectral reflectance spectrometry in the exploration for VMS deposits using the Izok Lake Zn-Cu-Pb-Ag deposit, Nunavut as a test site, In: Targeted Geoscience Initiative 4: Contributions to the Understanding of Volcanogenic Massive Sulphide Deposit Genesis and Exploration Methods Development, in: Peter, J.M., Mercier-Langevin, P. (ed.), Geological Survey of Canada, Open File 7853, 15–25.
- Laukamp, C., Cudahy, T., Thomas, M., Jones, M., Cleverley, J.S., Oliver, N.H.S., 2011. Hydrothermal mineral alteration patterns in the Mount Isa Inlier revealed by airborne hyperspectral data. *Australian Journal of Earth Sciences* 58, 917–936.
- Lee, C.M., Cable, M.L., Hook, S.J., Green, R.O., Ustin, S.L., Mandl, D.J., Middleton, E.M., 2015. An introduction to the NASA Hyperspectral Infrared Imager (HypSPIRI) mission and preparatory

- activities. *Remote Sensing of Environment* 167, 6–19.
- Le Maitre, R.W. (Ed.), 2002. *Igneous rocks. A classification and glossary of terms. Recommendations of the International Union of Geological Sciences Subcommittee on the Systematics of Igneous Rocks*, 2nd ed. Cambridge University Press, Cambridge.
- Livo, E.K., Johnson, M.R., 2011. Analysis of Imaging Spectrometer Data for the Aynak-Logar Valley Area of Interest. Chapter 2B. 40 p., in: Peters, S.G., King, T.V.V., Mack, T.J., and Chornack, M.P., eds., and the U.S. Geological Survey Afghanistan Mineral Assessment Team, 2011, *Summaries of important areas for mineral investment and production opportunities of nonfuel minerals in Afghanistan: U.S. Geological Survey Open-File Report 1*, 2011–1204.
- Lowell, J.D., Guilbert, J.M., 1970. Lateral and vertical alteration–mineralization zoning in porphyry ore deposits. *Economic Geology* 65, 373–408.
- Mars, J.C., Rowan, L.C., 2006. Regional mapping of phyllic-and argillic altered rocks in the Zagros magmatic arc, Iran, using Advanced Spaceborne Thermal Emission and Reflection Radiometer (ASTER) data and logical operator algorithms. *Geosphere* 2, 161–186.
- Mars, J.C., Rowan, L.C., 2011. ASTER spectral analysis and lithologic mapping of the Khanneshin carbonatite volcano, Afghanistan. *Geosphere* 7, 276–289.
- Mateer, M., 2010. Ammonium Illite at the Jerritt Canyon District and Gold strike Property, Nevada: its spatial distribution and significance in the exploration of Carlin-type deposits. Thesis (Master). University of Wyoming.
- Mitchell, R.H., 1986. *Kimberlites: mineralogy, geochemistry, and petrology*. Plenum Press, London.
- Momose, A., Miyatake, S., Arvelyna, Y., Nguno, A., Mhopjeni, K., Sibeso, M., Muyongo, A., Muvangua, E., 2011. Mapping pegmatite using HyMap data in southern Namibia. *IEEE International Geoscience and Remote Sensing Symposium (IGARSS)*.
- Nagal, S., 2013. Spectral analysis of Hyperion data for mapping the spatial variation of bauxite mineral in a part of Katni District, Madhya Pradesh, India. *International Journal of Scientific & Engineering Research* 4, 23–28.
- Neave, D.A., Black, M., Riley, T.R., Gibson, S.A., Ferrier, G., Wall, F., Broom-Fendley, S., 2016. On the Feasibility of Imaging Carbonatite-Hosted Rare Earth Element Deposits Using Remote Sensing. *Economic Geology* 111, 641–665.
- Ngcofe, L., Minaar, H., Halenyane, K., Chevallier, L., 2013. Multispectral and hyperspectral remote sensing: target area generation for porphyry copper exploration in the Namaqua Metamorphic province, South Africa. *South African Journal of Geology* 116.2, 259-272.
- Oshigami, S., Yamaguchi, Y., Uezato, T., Momose, A., Arvelyna, Y., Kawakami, Y., Miyatake, S., Nguno, A., 2013. Mineralogical mapping of southern Namibia by application of continuum-removal MSAM method to the HyMap data. *International Journal of Remote Sensing* 34, 5282-5295.
- Peter, J.M., Layton-Matthews, D., Gadd, M.G., Gill, S., Baker, S., Plett, S., Paradis, S., 2015. Application of visible-near infrared and short wave infrared spectroscopy to sediment-hosted zinc-lead deposit exploration in the Selwyn Basin, Yukon, in Paradis, S., ed., *Targeted Geoscience Initiative 4: sediment-hosted Zn-Pb deposits: processes and implications for exploration*; Geological Survey of Canada, Open File 7838, pp. 152-172.
- Pirajno, F., 2009. *Hydrothermal Processes and Mineral Systems*. Springer/Geological Survey of Western Australia, Dordrecht.
- Pollard, P.J., Taylor, R.G., Cuff, C., 1988. Genetic modeling of greisen-style tin systems, in: Hutchison, C.S. (Ed.), *The Geology of Tin Deposits in Asia and the Pacific*. Springer-Verlag, Berlin, pp. 59-72.
- Pour, A.B., Hashim, M., Pournamdari, M., 2015. Chromitite prospecting using Landsat and Aster remote sensing data. *ISPRS Annals of the Photogrammetry, Remote Sensing and Spatial Information Sciences, Volume II-2/W2*. Joint International Geoinformation Conference.
- Pour, A.B., Hashim, M., 2014. Alteration mineral mapping using ETM+ and Hyperion remote sensing data at Bau Gold Field, Sarawak, Malaysia. *8th International Symposium of the Digital Earth (ISDE8)*. IOP Conf. Series: Earth and Environmental Science 18, 1-5.
- Pour, A.B., Hashim, M., 2012. The application of ASTER remote sensing data to porphyry copper and epithermal gold deposits. *Ore Geology Reviews* 44, 1-9.
- Ridley, J., 2013. *Ore Deposit Geology*. Cambridge University Press, Cambridge.
- Riley, D., Hecker, C.A., 2013. Mineral mapping with airborne hyperspectral thermal infrared remote sensing at Cuprite, Nevada, USA, in: Kuenzer, C., Dech, S. (Eds.), *Thermal infrared remote sensing:*

- sensors, methods, applications, v. 17, Series Remote Sensing and Digital Image Processing, Springer, pp. 495-514.
- Riley, D., Cudahy, T., Hewson, R., Jansing, D., Hackwell, J., 2007. SEBASS imaging for Copper Porphyry and Skarn Deposits, Yerington, NV. Fifth Decennial International Conference on Mineral Exploration..
- Rivard, B., Zhang, J., Feng, J., Sanchez-Azofeifa, G.A., 2009. Remote predictive lithologic mapping in the Abitibi Greenstone Belt, Canada, using airborne hyperspectral imagery. *Canadian Journal of Remote Sensing* 35, S95–S105.
- Rockwell, B.W., Hofstra, A.H., 2008. Identification of quartz and carbonate minerals across northern Nevada using ASTER thermal infrared emissivity data—implications for geologic mapping and mineral resource investigations in well-studied and frontier areas. *Geosphere* 4, 218–246.
- Rogge, D., Rivard, B., Segl, K., Grant, B., Feng, J., 2014. Mapping of Ni-Cu-PGE ore hosting ultramafic rocks using airborne and simulated EnMap hyperspectral imagery, Nunavik, Canada. *Remote Sensing of Environment* 152, 302-317.
- Rowan, L.C., Kingston, M.J., Crowley, J.K., 1986. Spectral reflectance of carbonatites and related alkalic igneous rocks; selected samples from four North American localities. *Economic Geology* 81, 857–871.
- Rowan, L.C., Bowers, T.L., Crowley, J.K., Anton-Pacheco, C., Gumiel, P., Kingston, M.J., 1995. Analysis of airborne visible-infrared imaging spectrometer (AVIRIS) data of the Iron Hill, Colorado, carbonatite-alkali igneous complex. *Economic Geology* 90, 1966–1982.
- Rowan, L.C., Clark, R.N., Green, R.O., 1996. Mapping minerals in the Mountain Pass, California area using Airborne Visible – Infrared Imaging Spectrometer (AVIRIS) data. 11th Conference on Geologic Remote Sensing.
- Rowan, L.C., Mars, J.C., 2003. Lithologic mapping in the Mountain Pass, California area using Advanced Spaceborne Thermal Emission and Reflection Radiometer (ASTER) data: *Remote Sensing of Environment* 84, 350–366.
- Sabins, F.F., 1999. Remote sensing for mineral exploration. *Ore Geology Reviews* 14, 157–183.
- Sabins, F.F., 1997. *Remote Sensing — Principles and Interpretation*, 3rd ed., W.H. Freeman, New York.
- Salles, R.dosR., Souza Filho, C.R.de, Cudahy ,T., Vicente, L.E., Monteiro, L.V.S., 2017. Hyperspectral remote sensing applied to uranium exploration: A case study at the Mary Kathleen metamorphic-hydrothermal U-REE deposit, NW, Queensland, Australia. (*in press*). *Journal of Geochemical Exploration* 15.
- Salisbury, J.W., Walter, L.S., Vergo, N., D’Aria, D.M., 1991. *Infrared (2.1–2.5 µm) Spectra of Minerals*. Johns Hopkins University Press, Baltimore.
- Shau, G.A., Burke, H.K., 2003. Spectral imaging for remote sensing. *Lincoln Laboratory Journal* 14, 3-28.
- Spatz, D.M., 1996. Remote sensing strategies in mineral exploration and development: the precious metal and porphyry deposit models. *International Archives of Photogrammetry and Remote Sensing XXXI, Part B7*, 638–649.
- Suryanarayana Rao, K.V., Kumar, C., Kumar, A., Nandish, V., Swamy, R.T., 2013. Lamproites from the eastern margin of the Bhandara craton, Orissa, India: An Exploration Case Study, in Pearson, D.G. et al. (Eds.), *Proceedings of the 10th International Kimberlite Conference. Special Issue of the Journal of the Geological Society of India* 2, 129–141.
- Swayze, G.A., Clark, R.N., Goetz, A.F.H., Livo, K.E., Breit, G.N., Kruse, F.A., Sutley, S.J., Snee, L.W., Lowers, H.A., Post, J.L., 2014. Mapping Advanced Argillic Alteration at Cuprite, Nevada, Using Imaging Spectroscopy. *Economic Geology* 109, 1179-1221.
- Tangestani, M.H., Moore, F., 2002. Porphyry copper alteration mapping at the Meiduk area, Iran. *International Journal of Remote Sensing* 23, 4815–4825.
- Tappert, M.C., Rivard, B., Fulop, A., Rogge, D., Feng, J., Tappert, R., Stalder, R., 2015. Characterizing kimberlite dilution by crustal rocks at the Snap Lake diamond mine (Northwest Territories, Canada) using SWIR (1.90–2.36 µm) and LWIR (8.1–11.1 µm) hyperspectral imagery collected from drill core. *Economic Geology* 110, 1375-1387.
- Tappert, M.C., Rivard, B., Giles, D., Tappert, R., Mager, A., 2013. The mineral chemistry, near-infrared, and mid-infrared reflectance spectroscopy of phengite from the Olympic Dam IOCG deposit, South Australia. *Ore Geology Reviews* 53, 26–38.
- Taranik, J.V., Aslett, Z.L., 2009. Development of hyperspectral imaging for mineral exploration. *Reviews in Economic Geology* 16, 83–95.
- Taylor, G.R., Hansford, P., Stevens, B.P.J., Robson, D., 2005. HyMap™ of Broken Hill—imaging spectrometry for rock and mineral abundance mapping. *Exploration Geophysics* 36, 397–400.
- Thompson, A.J.B., Hauff, P.L., Robitaille, J.A., 1999. Alteration mapping in exploration; application of

- short-wave infrared SWIR spectroscopy. SEG Newsletter 39, 16–27.
- Thompson, A.J.B., Thompson, J.F.H., 1996. Atlas of alteration: a field and petrographic guide to hydrothermal alteration minerals. Geological Association of Canada, Mineral Deposits Division.
- Tukiainen, T., Thomassen, B., 2010. Application of airborne hyperspectral data to mineral exploration in North-East Greenland. Geological Survey of Denmark and Greenland Bulletin 20, 71–74.
- Tukiainen, T., Krebs, J.D., Kuosmanen, V., Laitinen, J., Schäffer, U., 2003. Field and laboratory reflectance spectra of kimberlitic rocks, 0.35–2.5 μm , West Greenland. Geological Survey of Denmark and Greenland, Report 43, 25.
- Tukiainen, T., Thorning, L., 2005. Detection of kimberlitic rocks in West Greenland using airborne hyperspectral data: the HyperGreen 2002 project. Geological Survey of Denmark and Greenland Bulletin 7, 69–72.
- Ungar, S.G., Pearlman, J.S., Mendenhall, J.A., Reuter, D., 2003. Overview of the Earth Observing One (EO-1) mission. IEEE Transactions on Geoscience and Remote Sensing 41, 1149–1153.
- Vane, G., Goetz, A.F.H., Wellman, J., 1984. Airborne Imaging Spectrometer: A new tool for remote sensing. IEEE Transactions on International Geoscience and Remote Sensing GE-22, 546–549.
- Vane, G., Green, R.O., Chrien, T.G., Enmark, H.T., Hansen, E.G., Porter, W.M., 1993. The Airborne Visible/Infrared Imaging Spectrometer (AVIRIS). Remote Sensing of Environment 44, 117–126.
- van der Meer, F., Hecker, C., van Ruitenbeek, F., van der Werff, H., Wijkerslooth, C., Wechsler, C., 2014. Geologic remote sensing for geothermal exploration: A review. International Journal of Applied Earth Observation and Geoinformation 33, 255–269.
- van der Meer, F.D., van der Werff, H.M.A., van Ruitenbeek, F.J.A., Hecker, C.A., Bakker, W.H., Noomen, M.F., van der Meijde, M., Carranza, E.J.M., de Smeth, J.B., Woldai, T., 2012. Multi- and hyperspectral geologic remote sensing: a review. International Journal of Applied Earth Observation and Geoinformation 14, 112–128.
- van Ruitenbeek, F.J.A., Cudahy, T., van der Meer, F.D., Hale, M., 2012. Characterization of the hydrothermal systems associated with Archean VMS-mineralization at Panorama, Western Australia, using hyperspectral, geochemical and geothermometric data. Ore Geology Reviews 45, 33–46.
- van Ruitenbeek, F.J.A., Cudahy, T., Hale, M., van der Meer, F.D., 2005. Tracing fluid pathways in fossil hydrothermal systems with near-infrared spectroscopy. Geology 33, 597–600.
- van Ruitenbeek, F.J.A., Debba P., van der Meer, F.D., Cudahy, T., van der Meijde, M., Hale, M., 2006. Mapping white micas and their absorption wavelengths using hyperspectral band ratios. Remote Sensing of Environment 102, 211–222.
- Vaughan, R.G., Hook, S.J., Calvin, W.M., Taranik, J.V., 2005. Surface mineral mapping at Steamboat Springs, Nevada, USA, with multi-wavelength thermal infrared images. Remote Sensing of Environment 99, 140–158.
- Vaughan, R.G., Calvin, W.M., Taranik, J.V., 2003. SEBASS hyperspectral thermal infrared data: surface emissivity measurement and mineral mapping. Remote Sensing of Environment 85, 48–63.
- Verplanck, P.L., van Gosen, B.S., Seal, R.R., McCafferty, A.E., 2014. A deposit model for carbonatite and peralkaline intrusion-related rare earth element deposits. U.S. Geological Survey Scientific Investigations Report 2010–5070-J, 58.
- Vincent, R.K., 1997. Fundamentals of Geological and Environmental Remote Sensing. Prentice Hall, New York.
- Walters, S.G., 1998. Broken Hill-type deposits. Journal of Australian Geology and Geophysics 17, 229–237.
- Wang, R., Cudahy, T.J., Laukamp, C., Walshe, J.L., Bath, A., Mei, Y., Young, C., Roache, T.J., Jenkins, A., Roberts, M., et al. 2017.
- White mica as a hyperspectral tool in exploration for Sunrise Dam and Kanowna Belle gold deposits, Western Australia. Economic Geology 112, 1153–1176.
- Watson, K., Kruse, F.A., Hummer-Miller, S., 1990. Thermal infrared exploration in the Carlin trend, northern Nevada. Geophysics 55, 70–79.
- Zadeh, M.H., Tangestani, M.H., Roldan, F.V., Yusta, I., 2014. Sub-pixel mineral mapping of a porphyry copper belt using EO-1 Hyperion data. Advances in Space Research 53, 440–451.
- Zamudio, J.A., 2009. Focusing field exploration efforts, using results from hyperspectral data analysis of the El Capitan gold-platinum group metals-iron deposit, New Mexico. Reviews in Economic Geology 16, 169–176.
- Zimmermann, R., Brandmeier, M., Andreani, L., Mhopjeni, K., Gloaguen, R., 2016. Remote Sensing Exploration of Nb-Ta-LREE-Enriched Carbonatite (Epeembe/Namibia). Remote Sensing 8, 620.